ELSEVIER

Catalysis Today 52 (1999) 249–258

CATALYSIS TODAY

www.elsevier.com/locate/cattod

The role of inter- and intra-phase mass transfer in the SCR-DeNO$_x$ reaction over catalysts of different shapes

Enrico Tronconi*, Alessandra Beretta

Dipartimento di Chimica Industriale e Ingegneria Chimica "G. Natta" del Politecnico di Milano,
P.zza Leonardo da Vinci 32, 20133 Milan, Italy

Abstract

The rate controlling role of gas/solid diffusive transport and of intraporous diffusion in SCR-DeNO$_x$ monolith (honeycomb and plate-type) catalysts is demonstrated and discussed in view of opportunities for catalyst optimization and process development. On the contrary, axial diffusion and pressure drop are shown to be negligible phenomena in typical SCR monolith reactors. © 1999 Elsevier Science B.V. All rights reserved.

Keywords: Mass transfer; SCR-DeNO$_x$ monolith; Catalyst optimization

1. Introduction

The goal of this paper is to illustrate and rationalize the role of mass-transfer limitations and of other physical phenomena in determining the behavior of gas/solid catalytic reactors, using the SCR-DeNO$_x$ process over monolith catalysts as an example. The reason for selecting this reaction is threefold:

1. Our research group has developed a long-time experience in its experimental and theoretical investigation [1,2].
2. As discussed in a previous contribution [3], this example seems particularly appropriate for teaching and introductory purposes, since it involves well-defined hydrodynamic (laminar flow) and geometrical (square monolith channels) aspects which afford simple but rigorous analysis.
3. The SCR-DeNO$_x$ process may serve as a useful introduction to the growing innovative subject of structured catalysts and reactors [4].

In the following we address the influence of mass-transfer limitations and of other physical phenomena on the SCR-DeNO$_x$ reaction over industrial-type honeycomb monolith catalysts. For both interphase and intraporous diffusion we present data proving the onset of such limitations, then we discuss how related critical parameters can be either estimated or measured in view of a quantitative analysis, and finally we show how mathematical modeling and simulation of the SCR monolith reactor provides practical guidelines for rationalization of experimental data, for process optimization and for catalyst design. The relevance of axial diffusion in the monolith channels, as well as of pressure drop, is likewise discussed. In this work the emphasis is not on the derivation of model equations; rather, we wish to show that the engineering analysis is informative of how the

---

*Corresponding author. Fax: +39-02-70638173
E-mail address: enrico.tronconi@polimi.it (E. Tronconi)

PII: S0920-5861(99)00079-6

geometry of the catalyst and the hydrodynamic regime affect the governing physical phenomena, resulting in different reactor performances in spite of similar intrinsic catalyst activities.

2. Background on the SCR-DeNO$_x$ process

Selective catalytic reduction (SCR) is now-a-days a world-wide implemented commercial technology for NO$_x$ abatement from power plant flue gases[1,2,5,6]. It is based on the reaction among nitrogen oxides (essentially nitrogen monoxide), ammonia and oxygen according to the following primary stoichiometry,

$$4NO + 4NH_3 + O_2 \rightarrow 4N_2 + 6H_2O \qquad (1)$$

Typical commercial SCR catalysts consist of TiO_2, WO_3 and V_2O_5 acting as the support, the promoter, and the active component, respectively. They are shaped in the form of honeycomb or plate-type monoliths: such structures afford low pressure drops and low tendency to clogging by ash and solid particles while retaining surface areas comparable to those of packed beds of catalyst pellets [1]. Incorporated honeycomb SCR catalysts consist of thousands of parallel channels of square cross section, with hydraulic diameters ranging from 3 mm (low-dust applications) up to 6 mm (high dust applications). Virtually isothermal operation of the SCR monolith reactors results from the negligible thermal effects associated with the very low reactant concentrations, typically 500 ppm or less.

Mechanistic and kinetic evidence is available to support the dominant role of strongly adsorbed ammonia in the reduction of gaseous or weakly adsorbed NO according to a Rideal reaction scheme [7–9]. As long as overstoichiometric feed ratios (α=NH_3/NO>1) are adopted, the overall kinetics of the SCR process are essentially first-order in NO and zero-order in NH_3 concentrations [10]. However, industrial reactors operate with substoichiometric feeds (α=NH_3/NO<1) to prevent emissions of unconverted ammonia: in this case the kinetic dependence on NH_3 must be considered. On the other hand, rate dependences on O_2 and H_2O content of the flue gases can be neglected as a first approximation under typical conditions [10].

It is now clearly established that the apparent kinetics of NO reduction by NH_3 over SCR monolith catalysts are actually the result of the interaction between the intrinsic reaction rate (very fast) and the (slower) diffusional transport of the reactants, occurring both from the bulk gas phase flowing inside the monolith channels to the catalytic walls (interphase mass transfer), and inside the porous monolith walls (intraporous diffusion). The next two sections are devoted to discussing such processes, respectively.

3. Interphase mass transfer

3.1. Phenomenological aspects

The flow regime prevailing in the channels of SCR honeycomb catalysts is laminar under the operating conditions of industrial interest, which involve linear velocities of the flue gases up to a few m/s. It is well known that laminar flow is less favorable than turbulent flow for interphase mass transfer, so we expect that the diffusive transport of the SCR reactants in DeNO$_x$ honeycombs from the bulk gas phase to the catalytic walls may be hindered to some extent. Since access of NO and NH_3 to the catalytic surface is in series to their conversion, this would adversely affect the overall performance of the monolith reactor. Fig. 1 presents literature data [11] of NO conversion vs. area velocity (AV=volumetric flow rate/catalyst geometric surface area) over two SCR honeycomb catalysts with the same chemical composition, but with different channel openings. A reduced overall activity is apparent for the catalyst sample with the greater channel hydraulic diameter, i.e. with the longer diffusion path length.

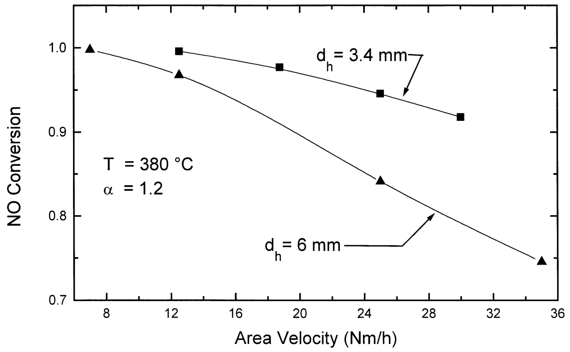

Fig. 1. Experimental effect of area velocity on NO conversion over two commercial SCR honeycomb catalysts with the same composition but different channel size. T=380°C, α=1.2 (data from Ref. [11]).

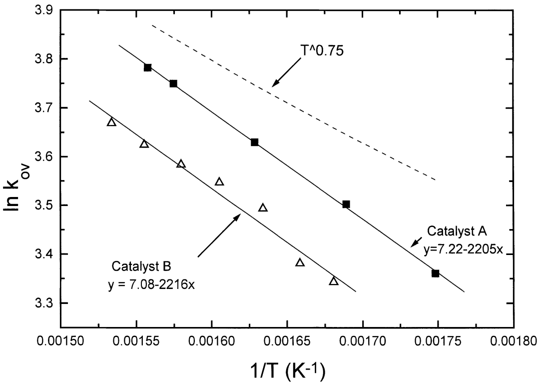

Fig. 2. Arrhenius plots for two commercial SCR honeycomb catalysts, compared with a power-law T-dependence=$T^{0.75}$. Catalyst A: α=1.1, AV=33 Nm/h, d_h=2.1 mm. Catalyst B: α=1.1, AV=26 Nm/h, d_h=4.9 mm.

Next we address the temperature dependence of the observed NO conversion data. Fig. 2 is an Arrhenius plot of the *overall* pseudo-first order rate constant k_{ov},

$$k_{\mathrm{ov}} = -\mathrm{AV}\ln(1 - x_{\mathrm{NO}}) \tag{2}$$

for two commercial SCR honeycomb catalysts, x_{NO} being the fractional conversion of NO. The estimates of the apparent activation energy provided by the slopes of the two straight lines through the data are both close to about 16 kJ/mol, a value much lower than expected for a catalytic reaction with rate controlled by chemical kinetics. On the other hand, Fig. 2 shows also that the measured slopes are in good agreement with a power-law T-dependence with exponent=0.75: this is characteristic of an external diffusion-limited regime, where the measured rate constant k_{ov} is proportional to the molecular diffusivity of NO in the gas stream ($\propto T^{1.75}$) and to the gas density ($\propto T^{-1}$).

Thus, both the observations that NO conversion: i) depends on the geometry of the monolith channels, and ii) exhibits a weak T-dependence, point out a significant role of gas–solid mass transfer in SCR honeycomb catalysts. Such a role must be properly accounted for in the analysis and simulation of SCR monolith reactors, at the industrial as well as at the laboratory scale. Quantitative treatment of gas–solid mass transfer in monoliths is the subject of the next section.

3.2. Evaluation of gas–solid mass transfer rates

If diffusion of the reactants from the bulk gas phase to the catalytic walls of the monolith channels is slower than their reaction, then the reactant concentrations at the wall, C_i^w are smaller than their average bulk concentrations in the gas phase, C_i^b. Adopting a simple 1D approach, neglecting axial diffusion (see Section 5.1 below), and assuming first-order kinetics, the steady-state differential mass balances of the reactants NO and NH$_3$ in the monolith channels (gas phase) and at the gas–solid interface (monolith walls) are, respectively [3]:

$$-u\frac{\mathrm{d}C_i^b}{\mathrm{d}z} = \frac{4}{d_h}k_{\mathrm{mt},i}(C_i^b - C_i^w), \quad i = \mathrm{NO},\ \mathrm{NH_3}, \tag{3}$$

$$k_{\mathrm{mt},i}(C_i^b - C_i^W) = k_{\mathrm{app}}C_i^w, \tag{4}$$

where u is the average flow velocity, k_{mt} is a mass-transfer coefficient and k_{app} is an apparent rate constant per unit monolith geometric area. Eqs. (3) and (4) are readily combined to give

$$-u\frac{\mathrm{d}C_i^b}{\mathrm{d}z} = k_{\mathrm{ov}}C_i^b \tag{5}$$

with the *overall* rate constant given by

$$\frac{1}{k_{\mathrm{ov}}} = \frac{1}{k_{\mathrm{mt}}} + \frac{1}{k_{\mathrm{app}}}. \tag{6}$$

Eq. (6) reflects the sequential arrangement of the *resistances* to gas–solid mass transfer and to the catalytic reaction. If chemical reaction is the slower process ($k_{\mathrm{app}} \ll k_{\mathrm{mt}}$), then $k_{\mathrm{ov}} \approx k_{\mathrm{app}}$ and we need not worry about the mass transfer coefficient k_{mt}. But if mass transfer is the rate controlling process ($k_{\mathrm{app}} \gg k_{\mathrm{mt}}$), then $k_{\mathrm{ov}} \approx k_{\mathrm{mt}}$, and we are faced with the problem of obtaining adequate estimates of the mass transfer coefficient k_{mt} in order to describe the reactor behavior.

The evaluation of mass (and heat) transfer coefficients for 1D models of laminar flow monolith reactors is still under debate. Both experimental and theoretical approaches have been proposed in the literature. The experimental method relies on running a very fast catalytic reaction (e.g. CO oxidation) over monolith catalysts of different length and size, and determining k_{mt} from conversion data using Eq. (5) and the assumption that $k_{\mathrm{ov}} \approx k_{\mathrm{mt}}$. Typical data are reported for example by Ullah et al. [12]. However, widely diverging results were published in the past; independent studies have shown in fact that accurate measurements of mass-transfer rates in monoliths under strictly diffusional control may be hard to obtain [13]. The most reliable results to date are probably those of Uberoi and Pereira [14]: based on data for the mass-transfer limited CO oxidation in square-channeled titania–silica honeycomb catalysts with the same geometric characteristics of industrial SCR-DeNO$_x$ monoliths, they proposed the following correlation for the *average* Sherwood number $Sh_{\mathrm{av}}=(k_{\mathrm{mt}}\ d_{\mathrm{h}}/D)$, i.e. a dimensionless mass-transfer coefficient averaged over the entire monolith length,

$$Sh_{\mathrm{av}} = 2.696[1+0.139/z^*]^{0.81} \tag{7}$$

with $z^* = LD/(d_h^2 u)$, a dimensionless axial length of the monolith catalyst.

The form of Eq. (7) recalls a semi-theoretical correlation proposed by Hawthorn [15], who introduced an empirical correction to the analogy between heat and mass transfer in laminar flow in square ducts in order to fit experimental data on honeycomb monoliths, resulting in

$$Sh_{\mathrm{av}} = 2.976[1+0.095/z^*]^{0.45}. \tag{8}$$

However, a fully theoretical approach involves the development of complete, rigorous multidimensional models of laminar-flow monolith reactors and the derivation of correlations for *Sh* from their numerical solutions. By this method Tronconi and Forzatti [16] have shown that *Sh* can be predicted according to the analogy between heat and mass transfer to laminar flow in ducts of constant wall temperature, a classical problem extensively treated in the engineering literature [17]. Their correlation for *local* Sherwood numbers in square channels with developing laminar flow is

$$Sh = 2.976 + 8.827(1000z^*)^{-0.545}\exp(-48.2z^*). \tag{9}$$

Eq. (9) was tested successfully against both steady-state and dynamic honeycomb SCR data obtained at the laboratory scale [8,18], and also against data collected in unsteady SCR-DeNO$_x$ of Diesel exhaust gases [19].

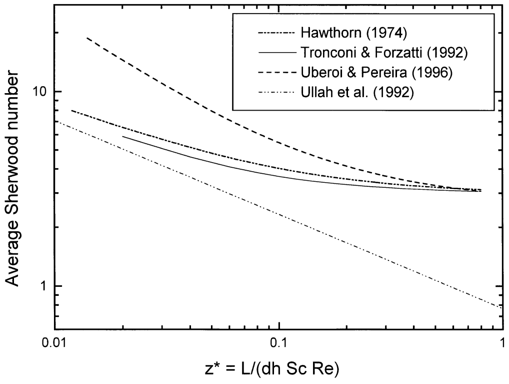

Fig. 3. Correlations for the average Sherwood number in honeycomb monoliths.

The three approaches, Eqs. (7)–(9), and the correlation by Ullah et al. [12] are compared in Fig. 3 in terms of length-averaged Sherwood numbers.

Fig. 3 indicates that the theoretical approach of Tronconi and Forzatti and the semi-theoretical correlation of Hawthorn are very close over the whole range of z^*-values of practical interest. The experimental correlation of Uberoi and Pereira yields consistently greater *Sh* numbers, but eventually converges to nearly the same asymptotic value. The Ullah et al. correlation is significantly lower than all the others. The deviations of the four curves in Fig. 3 are representative of the uncertainty still affecting estimation of mass-transfer coefficients in monolith honeycomb catalysts. One can speculate that: a) the low data of Ullah et al. were not representative of a completely diffusional regime [13]; b) the higher values of *Sh* measured by Uberoi and Pereira originate from uncontrolled hydrodynamic effects at the monolith entrance, involving e.g. localized eddies. In summary, the theoretical approach seems to provide more conservative estimates at the moment.

3.3. Modeling applications

Channel size of SCR honeycomb catalysts. Fig. 4 is a design plot for the selection of the area velocity (i.e. of the catalyst volume at a given feed rate) required to satisfy a specification of 2 ppm NH$_3$ slip using honeycomb catalysts with different channel hydraulic diameters. The results in the Figure, based

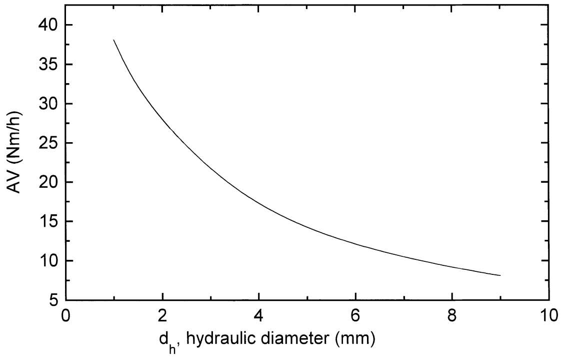

Fig. 4. Relationship between honeycomb channel diameter and area velocity providing 2 ppm NH_3 slip over a commercial SCR catalyst. T=380°C, α=0.8, C_{NO}^0=500 ppm.

on Eq. (9), point out the necessity of accounting for gas–solid mass transfer in the design of SCR reactors.

Honeycomb vs. plate-type SCR catalysts. In addition to honeycombs, there is a growing interest in the use of plate-type monolith catalysts for SCR-DeNO$_x$ processes, particularly for high-dust applications or where poor flue gas distribution and changes in load are probable. However, very little has been reported so far about gas–solid mass transfer in such structures. Their channel geometry [20] is considerably more complex than in square-channel honeycombs, making a theoretical approach more expensive. Giudici and Tronconi [21] have presented the analysis of heat transfer to fully developed laminar flow in plate-type monolith structures similar to a class of SCR catalysts. Because of the analogy between heat and mass transfer, their results, including correlations for the local Nusselt number, can be applied to the evaluation of gas–solid mass transfer coefficients (Sh numbers) in monolith catalysts with the same configuration. Fig. 5 compares the calculated performance of a high-dust honeycomb monolith and that of a plate-type monolith, for fixed catalyst properties. The plate-type configuration yields lower NO conversions. In fact, the industrial corrugated plates herein considered are characterized by a slower gas–solid diffusion rate (Sh_∞=2.14) than square ducts; also, the sinusoidal channels have wider cross sections and consequently a longer diffusion path than honeycombs, which further lowers the interphase diffusion rate of reactants.

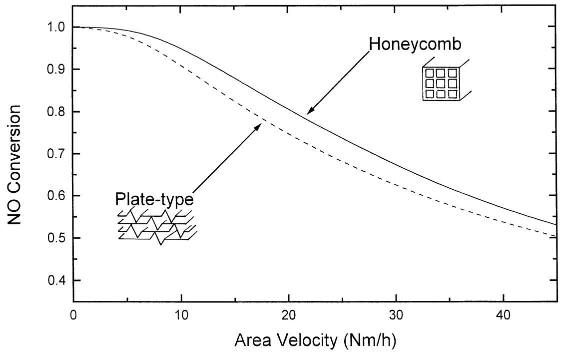

Fig. 5. Honeycomb vs. plate-type monoliths. α=1.1, C_{NO}^0= 500 ppm, T=350°C. $d_{h,\ \mathrm{honeycomb}}$=6.0 mm; $d_{h,\ \mathrm{plates}}$=8.4 mm. Interphase mass transfer in plate-type monoliths was estimated according to [21], case No. 4.

4. Intraporous mass transfer

4.1. Phenomenological aspects

In addition to the gas–solid mass transfer limitations discussed above, it is now well established that the SCR process suffers also from intraporous diffusional resistances which lower dramatically the catalyst utilization [7,22]. To better understand this aspect, let us reconsider the apparent rate constant k_{app} of a commercial SCR monolith: as shown by Eqs. (2) and (6), this can be estimated from NO conversion data after subtracting the contribution of inter-phase diffusion, k_{mt}. An example is provided in Fig. 6: the values of k_{app} herein plotted as solid square symbols were

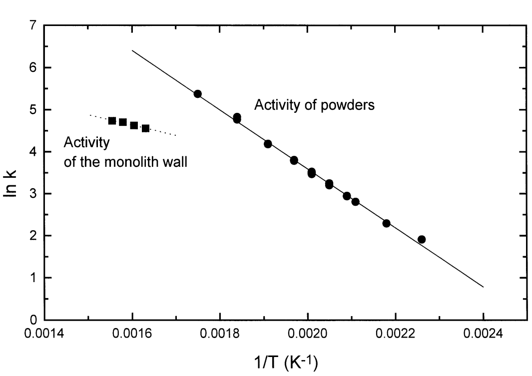

Fig. 6. Arrhenius plot of the apparent rate constant measured over a commercial SCR monolith catalysts (d_h=4.15 mm, t_w=0.8 mm) (squares) and over the same catalyst ground to particles (d=0.1 mm) (circles); α=1.1.

estimated by fitting Eqs. (5), (6) and (9) to NO conversion data obtained in our laboratories over a commercial SCR monolith with low-dust configuration (wall thickness=0.8 mm) in the 340–370°C temperature range. The estimate of the apparent activation energy amounted to nearly 29 kJ/mol. A sample of the same commercial monolith was then crushed into fine particles (average diameter≈0.1 mm) and their activity in the DeNO$_x$ reaction was measured in a fixed bed microreactor in the 200–300°C *T*-range. The data are given as solid circles in Fig. 6: they show that, when extrapolated to the industrial temperatures, the catalytic activity of the powders was markedly higher than the monolith activity. The temperature dependence of the rate constant over powders was also more pronounced, with an activation energy of about 59 kJ/mol. Such effects are associated with the influence of intraphase mass transfer: this was negligible in the fine particles but controlled the process rate in the monolith catalyst.

In the case of the small catalyst particles, the intraporous diffusion path was short enough to allow uniform access of the reactants to all the catalyst active sites. In the monolith walls, however, due to a much longer characteristic size, the rate of consumption of NO and NH$_3$ prevailed over the rate of diffusion of the same species inside the catalyst wall. The reactants were thus used up within a thin superficial layer of catalyst, while most of the inner catalyst wall remained inactive, being depleted of reactants. The average reaction rate across the wall half-thickness was therefore much lower than the reaction rate at the gas–solid interface.

Since the monolith wall can be approximated as an infinite slab, the following expression for the catalyst effectiveness factor is adopted [23]:

$$\eta = \frac{1}{\Phi} = \frac{1}{t_\mathrm{w}/2}\sqrt{\frac{D_\mathrm{eff,\,NO}}{k_\mathrm{c}}} \quad \text{with } \Phi \gg 1, \tag{10}$$

where Φ is a Thiele modulus, t_w the monolith wall thickness, $D_\mathrm{eff,\,NO}$ the effective intraporous diffusivity of NO, and k_c the intrinsic rate constant. Eq. (10) is valid for first-order kinetics, which applies to the special case of NH$_3$/NO feed ratios>1. A more complex expression for the effectiveness factor valid for Rideal kinetics over the whole range of feed compositions was developed by Tronconi et al. [8]. The relation between the apparent rate constant k_app (per unit catalyst surface, measured from monolith activity data) and the intrinsic rate constant k_c (per unit catalyst volume, measured over fine catalysts powders) is thus:

$$k_\mathrm{app} = \eta k_\mathrm{c}\frac{t_\mathrm{w}}{2} = \sqrt{k_\mathrm{c} D_\mathrm{eff,\,NO}} \tag{11}$$

and

$$E_\mathrm{act,\,app} = \tfrac{1}{2}E_\mathrm{act,\,c}. \tag{12}$$

Eq. (12) indicates that intraporous resistances affect also the temperature dependence of the SCR reaction over monoliths, as they lower the apparent activation energy by a factor of 2 with respect to the intrinsic activation energy of the DeNO$_x$ reaction measured over powders.

Thus, both the experience and the theoretical analysis assess that the prediction of the performance of a monolithic SCR catalyst requires the estimation of the effective diffusion coefficients of the reactants inside its porous walls, $D_{\mathrm{eff},i}$. This is a general problem of catalytic reaction engineering, for which many approaches have been proposed. In the case of SCR catalysts, which often exhibit bimodal pore size distributions, the so-called *random pore model* has been recommended in the literature. This is briefly described in the following section.

4.2. Evaluation of effective diffusivity coefficients

The Wakao–Smith *random pore model* [24] assumes that the porous medium is an agglomerate of micro-porous particles; the void space between adjacent particles would give rise, instead, to macro-porosity. This morphological model assumes that the overall diffusion process results from three contributions: the diffusion from macro-pores to macro-pores, the diffusion from micro-porous particles to micro-porous particles, and the mixed diffusion from macro-pores to micro-porous particles and vice-versa, respectively. The effective diffusivity coefficient is evaluated as the weighted average of the diffusion coefficients for each path, with weights given by the probabilities of the various mechanisms. The adequacy of the random pore model for the calculation of effective diffusion coefficients in SCR monolith catalysts was experimentally verified by Beeckman [25], who measured the effective diffu-

Table 1
Experimental and estimated values of $D_{\mathrm{eff,\,NO}}$ at 20°C [25]

Catalyst	$D_{\mathrm{eff,\,NO}}$ (cm^2/s), measured	$D_{\mathrm{eff,\,NO}}$ (cm^2/s), calculated
A (r_m=80 Å, r_M=2500 Å, ϵ_m=0.5, ϵ_M=0.014)	0.00452	0.0051
B (r_m=120 Å, r_M=2500 Å, ϵ_m=0.44, ϵ_M=0.021)	0.00726	0.0069
C (r_m=110 Å, r_M=2500 Å, ϵ_m=0.42, ϵ_M=0.014)	0.0051	0.0057

sion coefficient of NO through SCR catalyst walls using a non-conventional diffusion cell based on a single monolith channel. Some data are listed in Table 1. Catalysts A, B, C have different morphological characteristics; in particular, the highest diffusion coefficient was found for catalyst B, which was characterized by the highest void fraction of macropores. Table 1 also reports the estimates of the diffusion coefficient computed according to the random pore model. It can be observed that a good agreement between experimental and calculated values of $D_{\mathrm{eff,\,NO}}$ was achieved, with deviations below 10%.

Measured and calculated values of NO effective diffusivity confirm that intraporous diffusion of SCR reactants is extremely slow compared to molecular diffusion; in fact the effective diffusion coefficients of NO and NH_3 are over two orders of magnitude smaller than molecular diffusivities. Accordingly, the effectiveness factor of the monolith catalyst is very low, usually in the range 1–10%, indicating that most of the catalyst remains inactive.

4.3. Catalyst design

Catalyst pore structure. A complete model of the SCR monolith reactor which accounts for the role of reaction kinetics, interphase mass transfer, and intraporous diffusion can be effectively applied to the design and optimization of the monolith catalyst. An interesting case is the optimization of the catalyst morphological features. We briefly report the main results of the related published studies [7,22].

As already mentioned, recent SCR commercial catalysts often present bi-modal pore size distributions. In fact, micro-pores offer the highest resistance to intraporous diffusion but enhance the catalyst surface area, the opposite being true for macro-pores; thus, both kinds of porosity grant a function which is favorable to the overall process, and their co-existence results in a synergic effect. This is clarified in Fig. 7, where calculated NO conversion is plotted as a function of the amount of micro-pores for given catalyst intrinsic activity and total pore volume, and for three different micropore radii. Notably, the curves exhibit maxima. In fact, in correspondence with very low micro-pore fractions the catalyst surface area is high but the reactant diffusion coefficients are low; on the contrary, at high contents of macropores, intraporous diffusion is enhanced, but the catalyst surface area is much reduced. For the assumed conditions it was calculated that an optimal combination was granted by ϵ_m=0.25 and ϵ_M=0.45, which resulted in the maximum attainable NO conversion [22]. Of course, other factors, including above all mechanical resistance, must be considered as well in the design of the catalyst pore structure in addition to catalyst utilization.

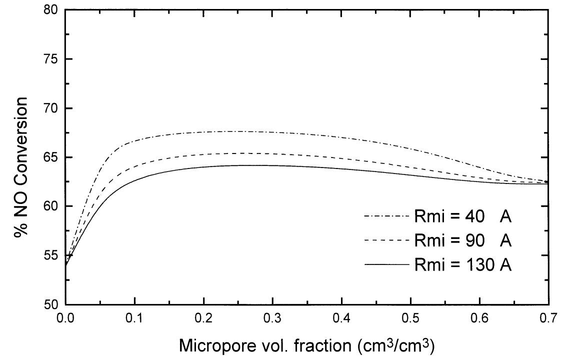

Fig. 7. Calculated influence of micropore fraction and radius on NO conversion.

Monolith wall thickness. It has been mentioned that commercial SCR monolith catalysts have very low effectiveness factors. Accordingly, the monolith wall thickness could be significantly reduced without affecting the DeNO$_x$ performance. For fixed operating conditions, catalyst activity and morphology, Fig. 8 shows that NO conversion is unaffected by decreasing the catalyst thickness down to a critical value corresponding to the depth of the superficial active layer.

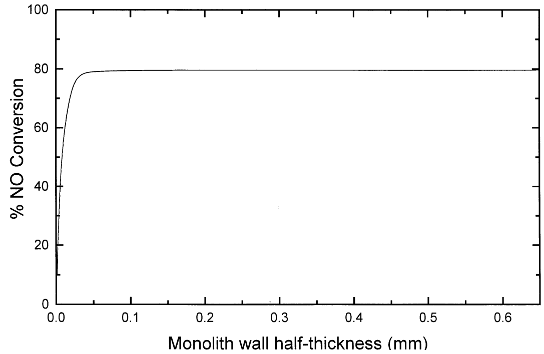

Fig. 8. Calculated effect of monolith wall thickness on NO conversion.

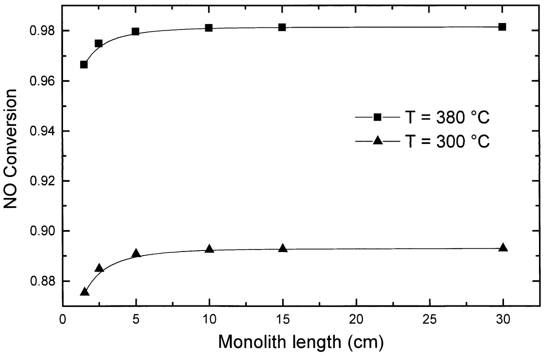

Fig. 9. Calculated effect of monolith length at constant AV=10 Nm/h. α=1.1, C^0_{NO}=500 ppm, d_h=6 mm.

5. Other physical phenomena

5.1. Axial diffusion

In principle, diffusive transport of the SCR reactants along the monolith channels due to their axial concentration gradients should be considered in addition to convective transport. In practice, this is generally neglected, primarily because such a contribution is often negligible, but sometimes also because it introduces significant mathematical complications in reactor modeling. To estimate the impact of such a simplifying assumption in the SCR case, NO conversions corresponding to different monolith lengths but constant area velocities were calculated taking into account axial molecular diffusion of NO and NH_3.

Sample results shown in Fig. 9 indicate that the influence of axial diffusion becomes appreciable only in the case of very short monoliths (L<5 cm).

It can be proven that this corresponds to a dimensionless criterion for significant axial diffusion effects based on the ratio of convective to diffusive process rates [26]:

$$\left(\frac{ud_h}{D}\right) < 10^2. \tag{13}$$

5.2. Pressure drop

Industrial SCR reactors contain up to four catalyst layers, usually about 1 m deep, with spacing in between. The gas stream flows in laminar regime inside the monolith channels, but turbulence and eddies arise between adjacent monolith layers. The pressure drop across each catalyst layer includes both the distributed contribution due to channel friction and the concentrated entrance/exit losses. It is usually evaluated according to an additive formula, such as

$$\Delta P = \frac{2f_m\rho u^2}{d_h}L + n\frac{\rho u^2}{2}. \tag{14}$$

The friction factor f_m for laminar flow in square channels is given by Shah and London [17]: f_m=14.227/Re. Concerning the contraction/expansion term, which is, however, much smaller, the expression n=1.75(1−ϵ) has been proposed for the coefficient in Eq. (14), ϵ being the monolith void fraction [27]; in the industrial practice entrance and exit losses for large-scale monoliths are simply accounted for by assuming n=1.5. Fig. 10(a) presents calculations of pressure drop across a 1 m catalyst layer vs. linear velocity of flue gases and monolith channel diameter. Typical values of linear velocity in high-dust SCR reactors amount to 3–5 m/s. It can be appreciated from the Figure that the monolith configuration is always associated with practically negligible pressure losses, even at the highest linear velocities and in the smallest channels. Notice also the virtually linear dependence of ΔP on gas velocity, typical of laminar flow, which confirms that the distributed loss is the dominant contribution. Fig. 10(b) reports the pressure drop per unit length across a packed bed of spheres, calculated according to the Ergun formula [23], as a function of linear velocity of the gas stream and of the sphere diameter.

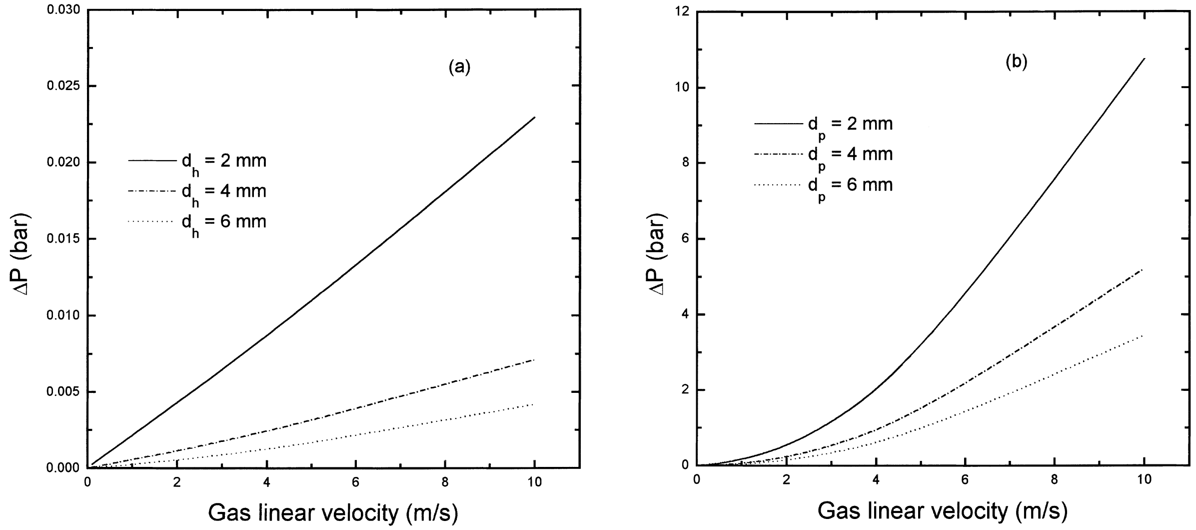

Fig. 10. Calculated pressure drop across: (a) 1 m deep layer of SCR honeycomb catalyst; (b) 1 m deep layer of spherical catalyst pellets. Effects of gas linear velocity and of channel diameter.

By comparison with Fig. 10(a), it is apparent that the use of packed beds is associated with pressure losses 2–3 orders of magnitude higher than in monoliths with equal characteristic size operated at the same linear velocity. This rules out the application of packed beds to the SCR–DeNO$_x$ treatment of power plant flue gases, which are emitted at atmospheric pressure and very high flow rates (10^6 Nm^3/h for a 300 MWatt power plant). In order to contain the pressure loss, a hypothetical packed-bed SCR reactor should be virtually two-dimensional with depth as short as possible and cross-section as wide as possible. Considering that, given the catalyst utilization and the surface-to-volume ratio of pellets, the removal of NO$_x$ from a medium size power plant would still require 50–100 m^3 of catalyst, this is clearly unrealistic.

6. Conclusions

Monolith catalysts for SCR-DeNO$_x$ applications, now-a-days a significant share of the market of industrial catalysts, typically operate under control of interphase and intraporous mass transfer. It is important to recognize the conceptual and quantitative implications of this fact for the following major reasons:

1. investigation of monolith catalysts at the laboratory scale yields data reflecting not only the intrinsic catalytic activity of the tested samples, but also their geometric configuration and pore structure;
2. catalyst development efforts can be more profitably directed towards optimization of the monolith pore size distribution, to improve the catalyst utilization, rather than to increasing the intrinsic activity, which is not the controlling factor under industrial conditions.

Engineering analysis shows that the performance of SCR monolith reactors is a complex function of design parameters and operating conditions, so that a purely empirical approach to optimization would be expensive and lengthy: this is indeed a case where mathematical modeling has proven an effective tool for process development work.

Finally, it is worth noting that the considerations on the important role of physical phenomena herein discussed for the SCR process similarly apply to other catalytic reactions based on monolith or structured catalysts, including e.g. catalytic combustion, methane partial oxidation, paraffin oxidative dehydrogenation. In these cases, however, the analysis becomes by far more complex due to the dominant heat transfer effects.

Acknowledgements

This work was performed under contracts with ENEL DSR-CRT, Pisa, and with ENEL-CRAM, Milano.

References

[1] P. Forzatti, L. Lietti, Heterog. Chem. Rev. 3 (1996) 33.
[2] A. Beretta, E. Tronconi, G. Groppi, P. Forzatti, in: J. Moulijn, A. Cybulski (Eds.), Structured Catalysts and Reactors, Chapter 5, Dekker, New York, 1998, p. 121.
[3] E. Tronconi, Catal. Today 34 (1997) 421.
[4] A. Cybulski, J.A. Moulijn, Structured Catalysts and Reactors, Dekker, New York, 1998.
[5] H. Bosch, F. Janssen, Catal. Rev. 2 (1988) 369.
[6] F. Nakajima, I. Hamada, Catal. Today 29 (1996) 109.
[7] J.W. Beeckman, L.L. Hegedus, Ind. Eng. Chem. Res. 30 (1991) 969.
[8] E. Tronconi, P. Forzatti, J.P. Gomez Martin, S. Malloggi, Chem. Eng. Sci. 47 (1992) 2401.
[9] L. Lietti, I. Nova, S. Camurri, E. Tronconi, P. Forzatti, AIChE J. 43 (1997) 2559.
[10] J. Svachula, N. Ferlazzo, P. Forzatti, E. Tronconi, F. Bregani, Ind. Eng. Chem. Res. 32 (1993) 1053.
[11] I. Binder-Begsteiger, G.W. Herzog, E. Megla, E.M. Tomann-Rosos, Chem.-Ing.-Tech. 62 (1990) 60.
[12] U. Ullah, S.P. Waldram, C.J. Bennett, T. Truex, Chem. Eng. Sci. 47 (1992) 2413.
[13] J. Villermaux, D. Schweich, Ind. Eng. Chem. Res. 33 (1994) 3025.
[14] M. Uberoi, C.J. Pereira, Ind. Eng. Chem. Res. 35 (1996) 113.
[15] R.D. Hawthorn, AIChE Symp. Ser. 137 (1974) 428.
[16] E. Tronconi, P. Forzatti, AIChE J. 38 (1992) 201.
[17] R.K. Shah, A.L. London, Laminar Flow Forced Convection in Ducts, Academic Press, New York, 1978.
[18] E. Tronconi, L. Lietti, P. Forzatti, S. Malloggi, Chem. Eng. Sci. 51 (1996) 2965.
[19] S.L. Andersson, P.L.T. Gabrielsson, C.U.I. Odenbrand, AIChE J. 40 (1994) 1911.
[20] M.V. Twigg, D.E. Webster, in: J. Moulijn, A. Cybulski (Eds.), Structured Catalysts and Reactors, Chapter 3, Dekker, New York, 1998, p. 59.
[21] R. Giudici, E. Tronconi, Int. J. Heat Mass Transfer 39 (1996) 1963.
[22] A. Beretta, E. Tronconi, L.J. Alemany, J. Svachula, P. Forzatti, in: V. Cortés Corberan, S. Vic Bellòn (Eds.), New Developments in Selective Oxidation II, Elsevier, Amsterdam, 1994, p. 869.
[23] G. Froment, K. Bischoff, Chemical Reactor Analysis and Design, 2nd ed., Wiley, New York, 1990.
[24] N. Wakao, J.M. Smith, Chem. Eng. Sci. 17 (1962) 825.
[25] J.W. Beeckman, Ind. Eng. Chem. Res. 30 (1991) 428.
[26] W.N. Gill, M.S. Suwandi, AIChE J 9 (1963) 273.
[27] J. Votruba, O. Mikus, V. Hlavacek, J. Skrivanek, Chem. Eng. Sci. 29 (1974) 2128.